Milsch, H. H., Spangenberg, E., Kulenkampff, J., Meyhöfer, S. (2007): A new apparatus for long-term petrophysical investigations on geothermal reservoir rocks at simulated in-situ conditions. - Transp Porous Med, 74, 1, 73-85

DOI: 10.1007/s11242-007-9186-4.

A new Apparatus for Long-term Petrophysical Investigations on Geothermal Reservoir Rocks at Simulated In-situ Conditions

H. Milsch[1], E. Spangenberg[1], J. Kulenkampff[1,2], and S. Meyhöfer[1]

[1] GeoForschungsZentrum Potsdam, Telegrafenberg, D-14473 Potsdam, Germany, milsch@gfz-potsdam.de
[2] now at Institut für Interdisziplinäre Isotopenforschung, Permoserstr. 15, D-04318 Leipzig, Germany

Abstract. We present a new apparatus capable of maintaining in-situ conditions pertinent to deep geothermal reservoirs over periods of months while in the same time allowing for a variety of continuous petrophysical investigations. Two identical devices have been set up at the GFZ-Potsdam.
Lithostatic overburden- and hydrostatic pore pressures of up to 100 and 50 MPa, respectively can be simulated. In addition in-situ temperature requirements of up to 200 °C can be met. The use of corrosion resistant parts throughout the pore pressure system allows investigations with highly saline formation fluids. Rock permeability, electrical conductivity as well as compressional- and shear-wave velocities can be measured simultaneously and the pore fluid can be sampled under pressure for further chemical analysis.
Scientifically, the usage of the device focusses on risk potentials in exploration and exploitation of deep geothermal reservoirs. Particularly, the investigations address possible effects of fluid-rock interactions on the transport properties of a reservoir host rock.

Key words: permeability, electrical conductivity, compressional- and shear-wave velocities, experimental petrophysics, fluid-rock interactions, geothermal reservoirs

1. Introduction

For the sustainable use of geothermal energy the reservoir, once put into operation, has to maintain its productivity over several decades. Besides an immediate formation damage at the stage of drilling (e.g. due to an improper filter-cake removal) the latter could be affected through numerous fluid-fluid- and fluid-rock interactions induced in the course of reservoir stimulation and exploitation (e.g. Civan, 2000). Their individual mechanisms can be of both mechanical and chemical origin (Leone and Scott, 1988). The former are mainly associated with the migration of fines like clay particles leading to pore throat plugging (e.g. Mader, 1989). The latter are generally related to changes in local chemical (thermodynamic) equilibrium. In addition to clay swelling (Omar, 1990; Tichstiakov, 2000) so induced dissolution-precipitation reactions of various kinds (e.g. Tenthorey et al., 1998; Sorbie and Mackay, 2000; Pape et al., 2005) can significantly affect the permeability of a reservoir host rock both near the wellbore and within the formation.
Despite scaling limitations and in terms of process-oriented studies laboratory investigations are a valuable complementary method of forecasting the physical consequences of such effects. Besides the selection of an appropriate sample material, testing under realistic in-situ conditions is necessary. This also includes the use of the respective formation fluids as well as a continuous fluid flow through the specimen. In addition, as an evolution of the rock transport properties depends on the rates of the transformations involved, stable experimental conditions have, eventually, to be maintained over longer time periods. Finally, it is desirable not only to measure changes in the petrophysical transport properties (e.g. permeability) but one should also be able – for explanatory purposes – to complement these investigations with pore fluid sampling and an analysis of the fluid chemistry.
Experimental high-pressure high-temperature machinery in earth-materials sciences is designed and laid out depending on the specific scientific scope in question. Conventional hydrothermal equipment used in petrology and mineral physics (autoclaves, piston-cylinder

apparatuses, etc.) is by all means unsuitable for the present purpose due to the small sample sizes and / or the lack of an independent pore pressure control. On the other hand, the potentially more suitable rock mechanics apparatuses (e.g. Paterson, 1990; Tenthorey et al., 1998; Heiland, 2003), even with an added-on pressure vessel and pore fluid system, have limitations regarding their long-term performance (e.g. a risk of hydraulic pump failure), the temperature range (either too low or too high), the quantity or type of fluid that can be handled and / or the required continuous fluid flow. In addition they do generally not offer the potential of measuring several petrophysical parameters at the same time. To meet the requirements stated above two identical devices have been set up at the GFZ-Potsdam being a refined derivative of an older concept described by Kulenkampff et al. (2005).
Our scientific objectives are a laboratory based petrophysical characterisation of deep geothermal systems as well as investigations on their potential alteration over time by processes induced in the course of reservoir exploration and exploitation.

2. Details of the experimental set-up

The general set-up of the apparatus is shown in Figure 1. A detailed description of the different components is given below. Design and assembly have been performed in-house. Also, various parts to the pressure vessel and the specimen assembly were manufactured at the GFZ-workshop. Other devices were purchased from different commercial suppliers.
A general view of the apparatus can be seen on Figure 2 from the pressure vessel side and Figure 3 from the pore fluid pump side.

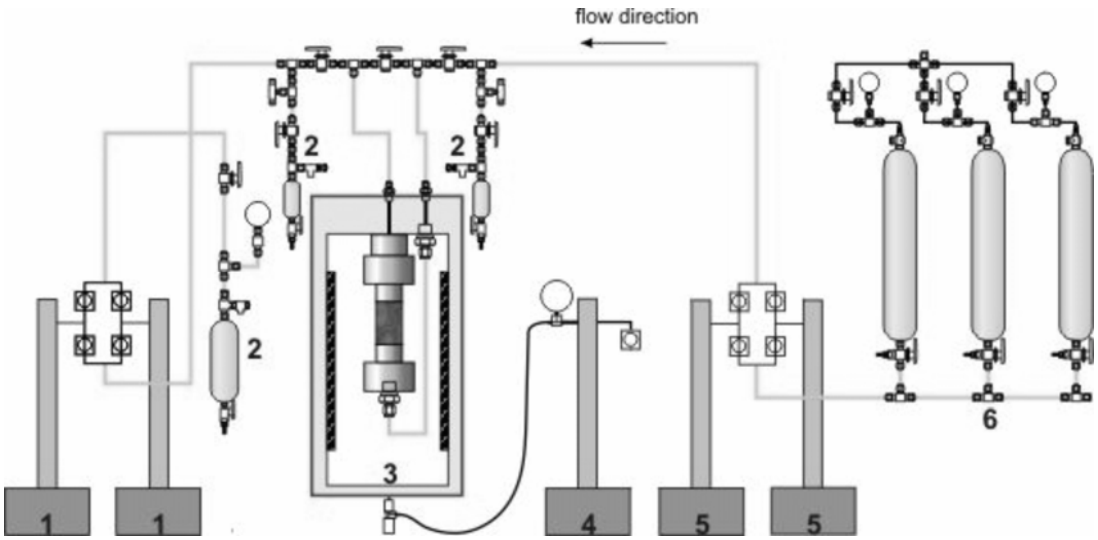

Figure 1. General set-up of the apparatus: (1) and (5) down- and upstream pore fluid pumps, respectively; (2) reservoirs for fluid sampling; (3) pressure vessel with internal heater and specimen assembly; (4) confining pressure pump; (6) fluid reservoir.

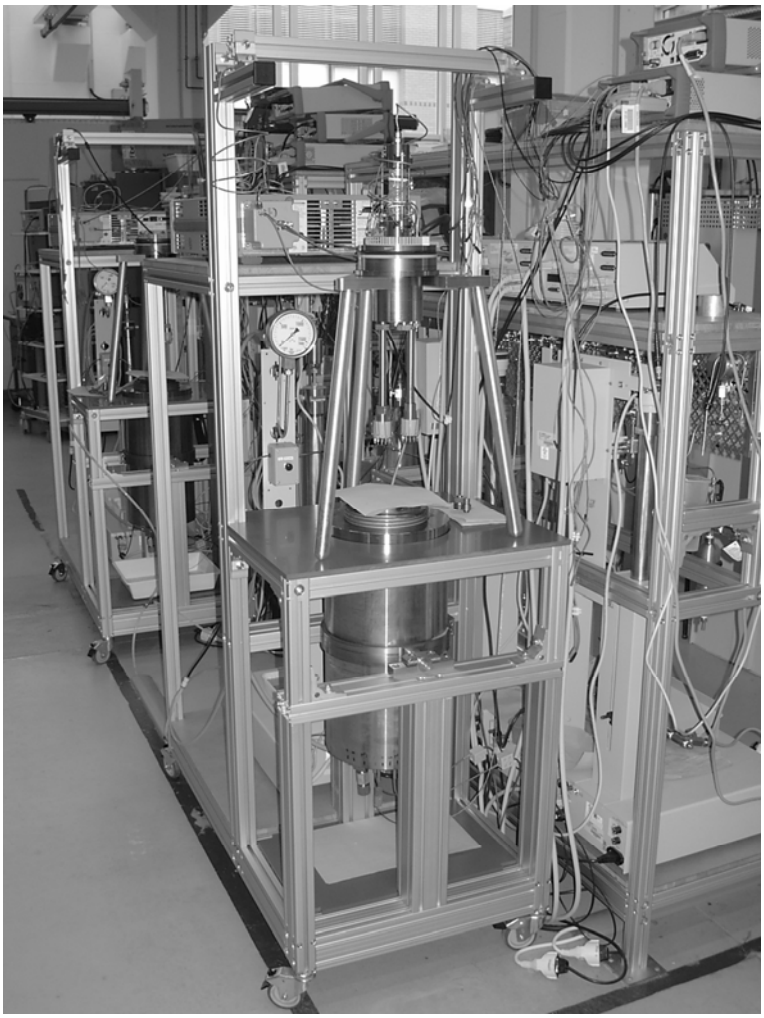

Figure 2. General view: Pressure vessel rack. The second identical apparatus can be seen behind.

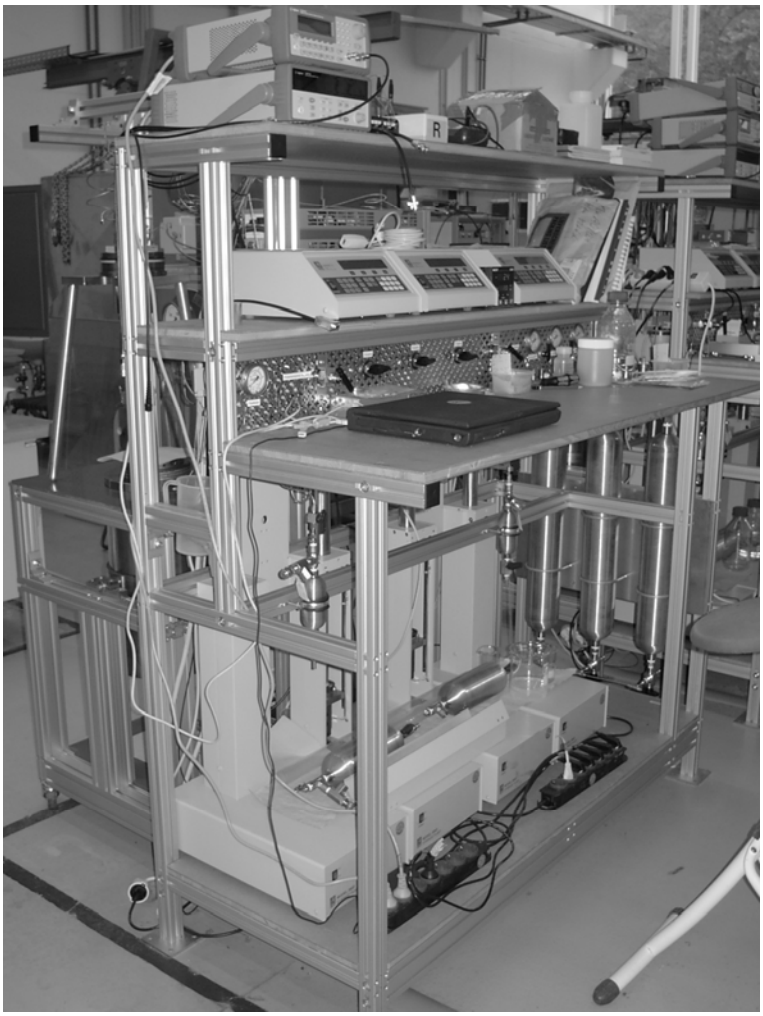

Figure 3. General view: Pore fluid pump rack with pump controllers and data aquisition above.

2a. Pressure vessel and confining pressure generation

The stainless steel pressure vessel (Number 3 in Figure 1) was custom made by Voggenreiter, Mainleus, Germany. It has a free internal volume of approximately 3500 mL and is officially certified to 140 MPa at 200 °C. The vessel is closed with one steel plug and one steel screw on either side. Each of the plugs has a certain number of bores for the feed-throughs of the heater and the specimen assembly described in more detail in the respective sections. The plugs are sealed against the atmosphere with one Viton 80 Shore O-ring backed by a PEEK miter-ring.
Conventional hydraulic oil is used as the confining pressure medium. Confining pressure is generated with one high pressure syringe pump with a full stroke internal volume of 68 mL (Isco 65D; Number 4 in Figure 1). The maximum operational pressure of the pump is 138 MPa (20000 psi). One full stroke corresponds to a pressure increase (decrease) of 20 MPa within the vessel or an expansion (contraction) compensation of the oil due to a temperature increase (decrease) of 30 °C. Thus, for higher pressure or temperature intervals the pump has to be emptied or refilled several times into or from a connected oil reservoir. Connection to the pressure vessel is realized by a high pressure hose (Spir Star). The vessel and the pump

are secured by an adequate burst disc connected to the hose (Sitec). Air-driven check valves (Isco) allow a controlled oil flow in either direction and thus pressurization and oil release. Both the pump and the valves are directly operated by an electronic servo controller unit supplied by the pump manufacturer. The servo controlled confining pressure as measured with the connected pressure gage (Honeywell) is stable to ± 0.05 MPa, the noise of the transducer being significantly lower (± 0.002 MPa).

2b. Heating device and temperature maintenance

Heating of the oil is performed by a resistance heating element (Thermocoax) mounted on a cylindrical stainless steel tube placed into the pressure vessel. In addition, a Type-K thermocouple coiled around the heater is used for temperature control. Electrical connections are made through the bottom plug by cylindrical feed-throughs made from stainless steel. The tubular heater- and thermocouple connectors are then gripped by fittings (Swagelok) to the feed-throughs which themselves are sealed against the atmosphere by one Viton 80 Shore- and one Teflon O-ring. The bottom plug of the vessel remains in place at all times unless some kind of maintenance would be necessary.
The heater is operated by a DC-power supply (Agilent 6675A) and a conventional external controller (West 4200). DC-powered heating was chosen to avoid introduction of electrical noise which would interfere with all measurements. Heating from room temperature to 200 °C is complete within approximately four hours. In contrast, cooling from 200 °C to room temperature takes 24 hours due the large volume of the pressure vessel. The former temperature is the technical limit in view of the long-term stability of the O-rings used within the device. The set temperature as measured within the vessel is stable to ± 0.5 °C, besides during times of confining pressure increase or decrease.

2c. Pore fluid system and pore pressure generation

The pore fluid system consists of several reservoirs, tubings, fittings and valves as well as a total of four syringe pumps. Fluids of different compositions can be stored in three stainless steel bottles (Swagelok; Number 6 in Figure 1) with a volume of 3000 mL each. A Teflon coat on the internal walls acts as a protective layer against corrosion. The tanks can be individually pressurized to 12 MPa thus allowing the stabilization of dissolved gases. Stainless steel type fractional 1/8'' OD tubing and corresponding fittings and valves (Swagelok) are used throughout the device. By the use of several valves various parts of the pore pressure system including the sample can be sealed off. The latter can also be bypassed by the fluid.
The four pore fluid pumps (Isco 260D; Number 1 and 5 in Figure 1) allow a continuous fluid flow through the sample. The individual full stroke volume is approximately 265 mL and the maximum operational pressure is 52 MPa (7500 psi). During flow one pump on either side of the sample is on hold under pressure and takes over when the other one has to be refilled (upstream) or emptied (downstream). An endless fluid flow can thus be maintained. All pumps can be independently run in both constant pressure- and constant flow mode. The latter can be varied from 10^{-3} to 107 mL/min. Fluid expulsion and -refill is accomplished by a pair of electric valves (Isco) attached to each pump. As for confining pressure generation, both the pumps and the valves are directly operated by an electronic servo controller unit supplied by the pump manufacturer. A total of two pumps and four valves are connected to one controller. The rate at which the pump adjusts changes in target pressure defined by the operator can be limited electronically. This allows pore pressure ramping at a preset rate. Each pump

possesses its own pressure gage mounted on top of the pump cylinder. Pore pressure stability will be discussed in more detail in Section 3 in connection with the permeability measurements. Syringe pumps were chosen for their slow, quasistatic (isothermal, isobaric) operation which minimizes variations of the thermal state of the fluids. In addition, they provide an excellent volumetric resolution.
Two stainless steel and Teflon-coated smaller reservoirs (Swagelok; Number 2 in Figure 1) allow sampling of the pore fluid under pressure both up- and downstream. The fluid is released by needle-valves to prevent disturbance of the pore pressure level. The reservoirs allow a fluid pressure of up to 12 MPa and are secured by proportional relief valves. The volume of each container is approximately 200 mL. Finally, after passing the downstream pumps, the fluid is released into a similar tank with a volume of 1000 mL.
The pore fluid system can easily be adjusted to changes in experimental strategy. For example return flow can be accomplished with minor modifications. Also a repeated pumping of the fluid that has transversed the sample would be possible. Finally, both apparatuses could be joined to simulate a geothermal doublet.

2d. Specimen assembly and sensors

The individual parts of the specimen assembly are shown in Figure 4. The sample is 30 mm in diameter and 40 mm in length. For the electrical conductivity measurements silver rims are painted onto the sample at a distance of 25 mm.
The specimen is sandwiched between two stainless steel plugs having a 2.0 mm ID concentrical bore and a machined grid on the touching side for fluid distribution (Figure 5a). FEP heat shrink tubing (Georgi I.V.) with 1.25:1 shrink ratio and 0.51 mm wall thickness is used as the jacket material. In general, two such tubings are used. The inner one is perforated to allow a silver foil strip to be connected to the silver rims. The second one seals the perforation by sqeezing a layer of silicone rubber into the void between the two jackets.
Ultrasonic measurements are performed with piezoelectric ceramics (Stelco, type P850 and PPK62, Curie temperature = 360 °C and 320 °C) for both compressional- (p) and shear- (s) waves, respectively. The sensors are arranged star-like and are adhered directly onto the plugs with epoxy (Figure 5b). Thus, wave velocities are determined in the core direction where one plug acts as the emitter, the other one as the passive receiver. A total of two piezos for the p- and six piezos for the s-waves are mounted on either plug. Electrical connections are made independently for p- and s-waves by wires soldered to the ceramics. In addition, a protective coating with ceramic cement is applied.
Sealing of the various parts of the assembly is made with Viton 80 Shore O-rings. The assembly is mounted onto the top plug of the pressure vessel and is connected with spring-shaped tubing used for pore fluid supply to the sample. This tubing has a length of approximately one meter and refers to the upstream side of the sample. The fluid is thus preheated to the oil temperature within the vessel before it enters the sample.
Electrical connections are made from the assembly to a PEEK-ring with a total of 48 sockets. From there insulation-coated copper wires are fed out of the pressure vessel. The feed-throughs are made from high pressure steel tubing (Sitec) filled with epoxy (Araldite) which is backed by a PEEK-wedge held by a stainless steel nut. A total of four such feed-throughs can be connected to the top plug of the vessel containing twelve copper wires each. The feed-throughs have been tested successfully to 100 MPa confining pressure.
Typically, one feed-through is used for connections to the top side of the sample and one for the bottom side. To each side of the specimen connections are made for mass, electrical potential, p- and s-wave piezos and a PT-100 RTD (Resistance Temperature Detector) for temperature measurements close to the sample.

Figure 6 shows a full set-up with the top plug in the center and the tubular feed-throughs below. A detail of the specimen assembly mounted onto the plug is shown in Figure 7.

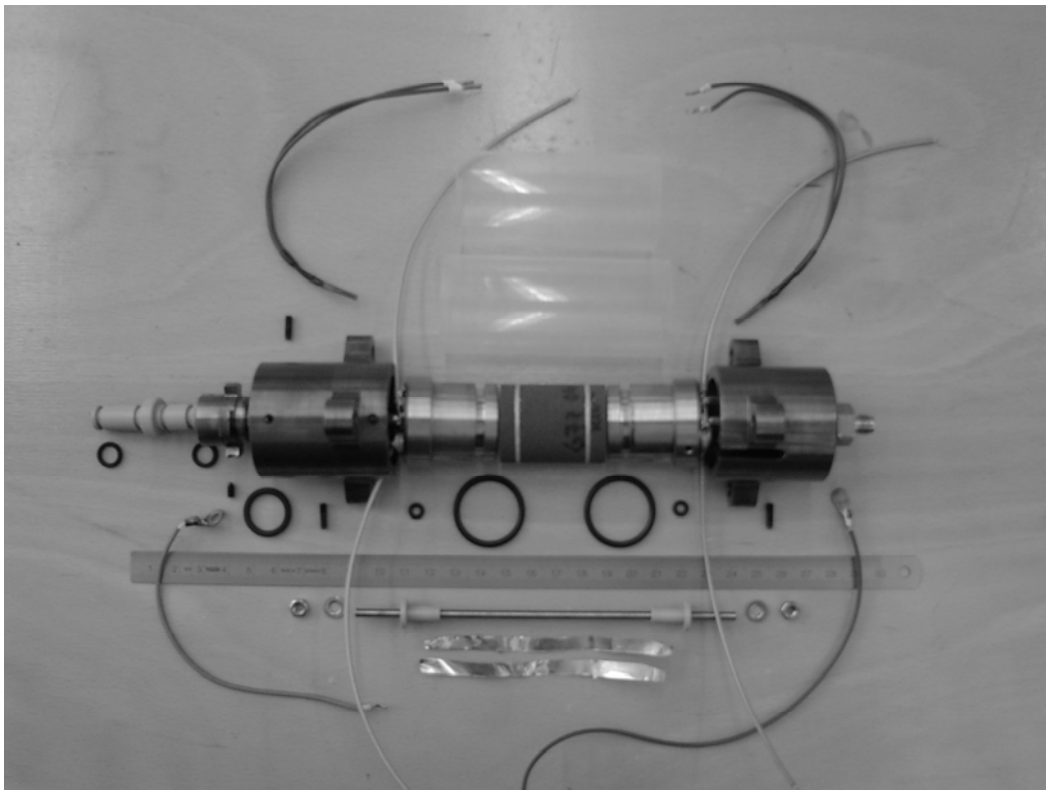

Figure 4. Parts of the specimen assembly. Silver rims painted onto the sample serve for measuring electrical conductivity.

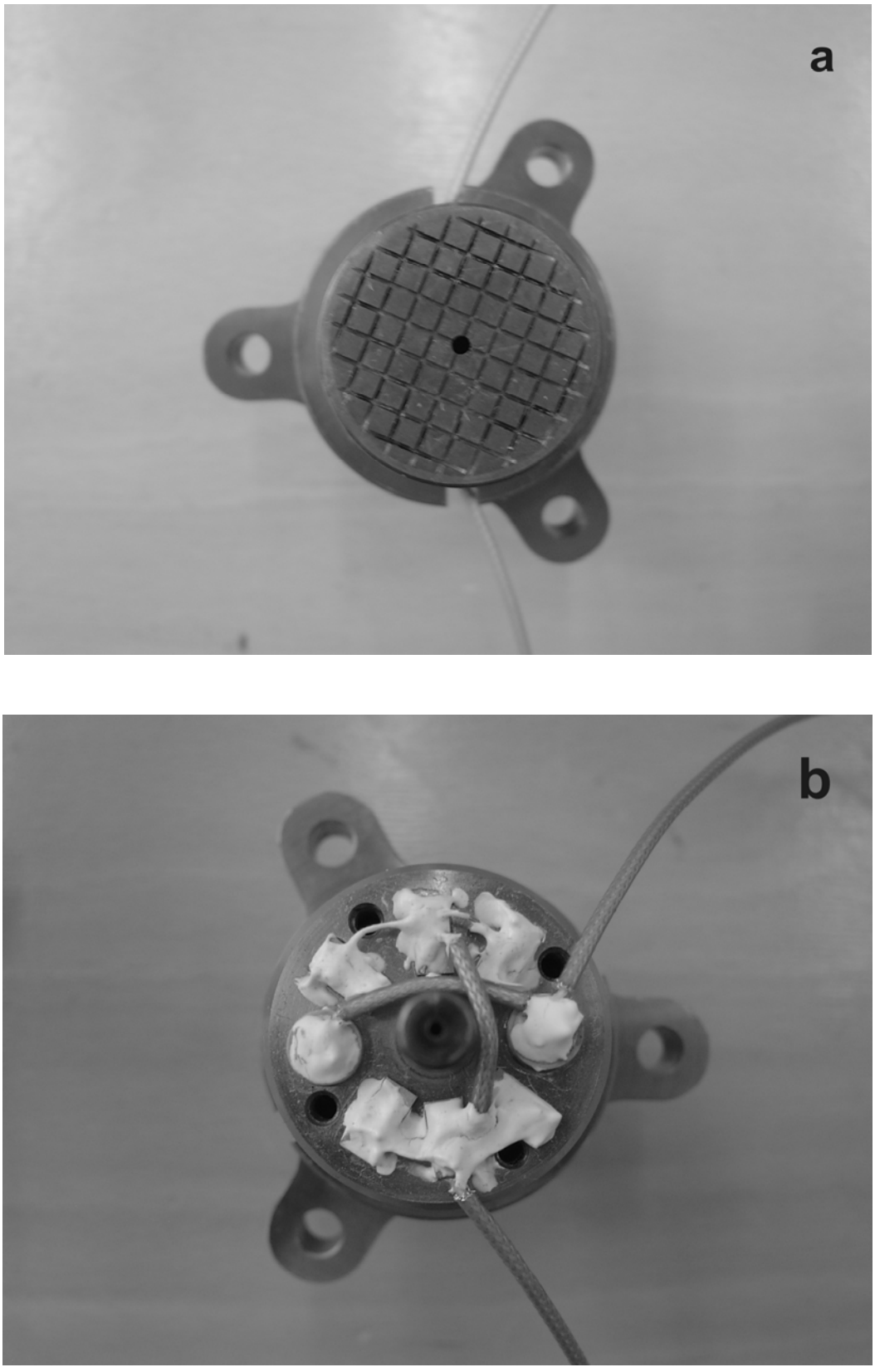

Figure 5. Specimen assembly steel plugs with a grid for fluid distribution (a) and piezos for ultrasonic measurements (b).

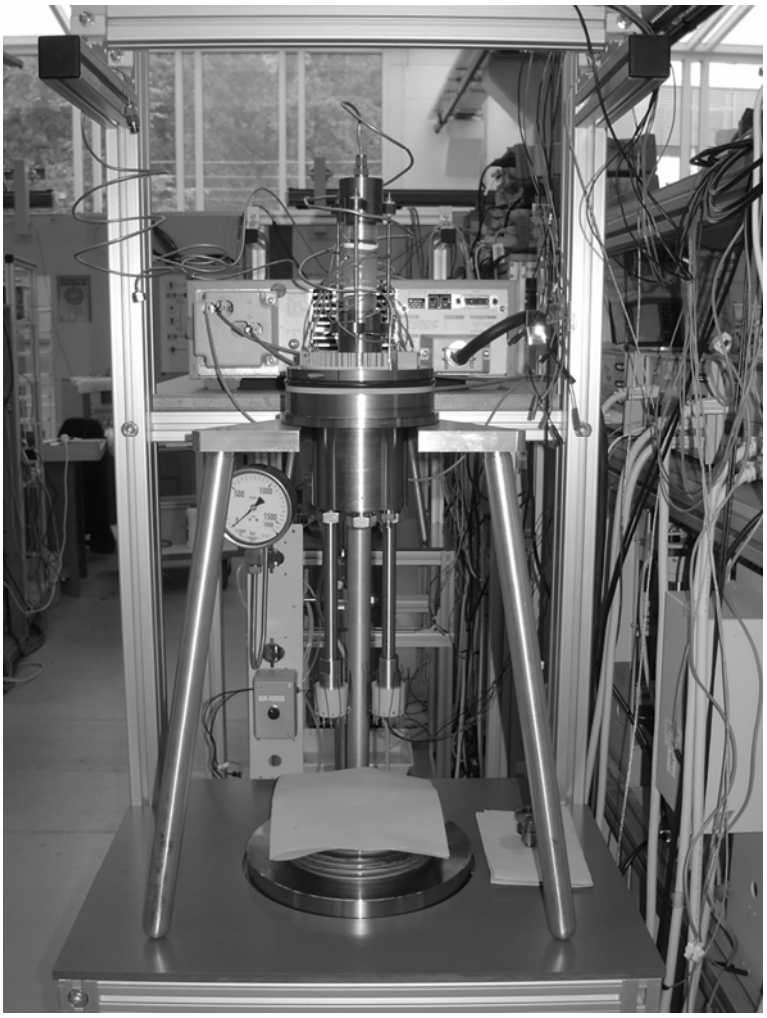

Figure 6. Top plug of the vessel (center) with tubular feed-throughs below.

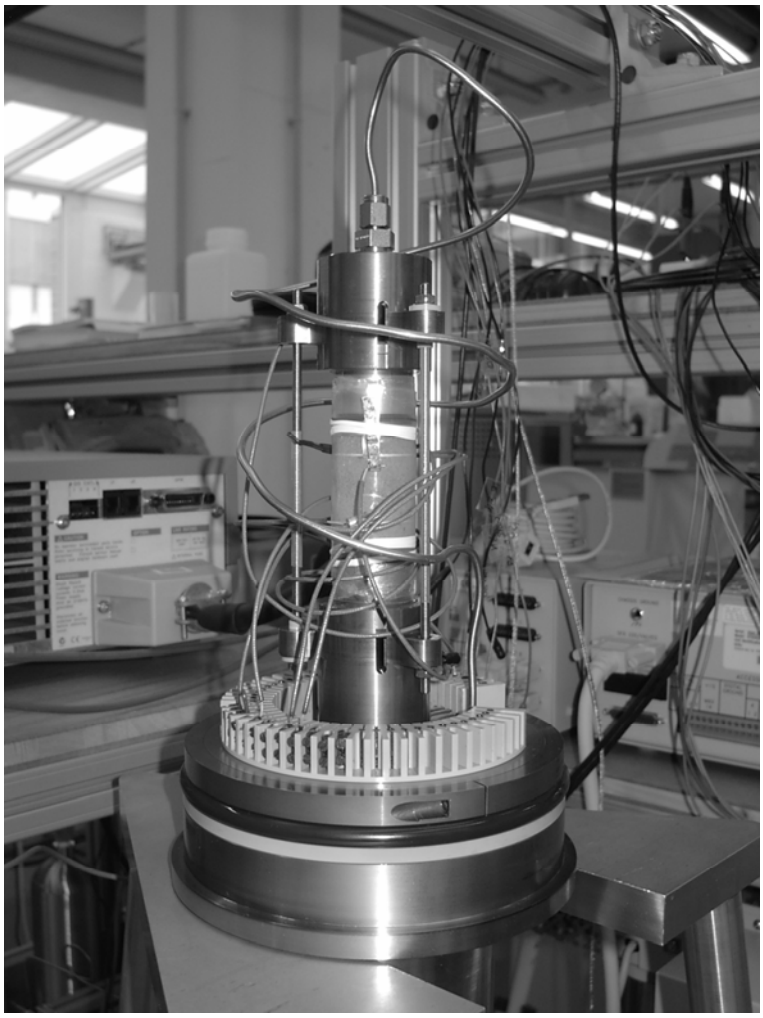

Figure 7. Detail of the mounted specimen assembly.

2e. Signal generation and data acquisition

For the electrical conductivity- and ultrasonic measurements voltage signals are impressed with a function generator (Agilent 33220A). Typically, the voltage is an AC-sine 1.0 V peak-to-peak signal at a frequency of 13 Hz and a rectangular voltage single burst at 1.0 V and 400 kHz for conductivity- and ultrasonic measurements, respectively. The generated ultrasonic excitation is amplified (Amplifier Research 50A220) before entering the sample and the received p- or s-waves are recorded by a two-channel digital oscilloscope (Agilent 54621A).
As electrical conductivity- and ultrasonic measurements use the same mass with respect to the sample, logging has to be performed consecutively. To facilitate a change in the respective connections the wires have been joined to a switch box.
Ultrasonic data is copied directly from the oscilloscope screen and stored on a floppy disc. All other signal lines for temperature, pressure and electrical conductivity are connected to a data acquisition and switch unit (Agilent 34970A). There, data scanning is performed in preset time intervals and the collected data is sent to a data acquisition program (Agilent Data Logger II) run on a notebook for further processing.

3. Petrophysical measurements and performance characteristics

3a. Permeability measurements

The permeability k of a rock is determined by a steady state method making direct use of Darcy's Law (e.g. Darcy, 1856; Scheidegger, 1974; Bear, 1988), thus assuming low Reynolds number (laminar) flow:

$$k = \frac{q \cdot \eta \cdot \Delta l}{\Delta p}, \tag{1}$$

where q, η, Δl and Δp denote, in this order, the fluid volume flux (the Darcy velocity), the (dynamic) fluid viscosity, the sample length and the pressure difference. Thus, permeability can be calculated for a known sample geometry and a specific flow-rate by the measured pressure gradient when the fluid viscosity is corrected for the individual temperature. The Reynolds number Re is defined as:

$$Re = \frac{\rho \cdot v \cdot l}{\eta}, \tag{2}$$

where ρ, v, l and η denote, in this order, the fluid density, the average fluid velocity within the pore space, the characteristic length (the pore dimensions) and the (dynamic) fluid viscosity. The velocity v can be related to the given Darcy velocity q by a law attributed to Dupuit and Forchheimer (e.g. Guéguen and Palciauskas, 1994):

$$v = \frac{q}{\varphi}, \tag{3}$$

where φ denotes the sample porosity. Re can then be estimated for the present flow situation: for pure water at 150 °C, a pore dimension of 10 µm, a porosity of 10 %, a sample diameter of 30 mm and a flow-rate of 1.0 mL/min one obtains Re = 0.012. Thus, if turbulence is assumed for Re >> 1 (Guéguen and Palciauskas, 1994, p. 120) Darcy's Law should be reasonably applicable up to the highest flow-rates and / or permeabilities accessible with the present device.

For flow stability reasons, continuous flow experiments are usually performed with the upstream pumps (Number 5 in Figure 1) in constant flow mode while the downstream pumps (Number 1 in Figure 1) are kept in constant pressure mode. The noise of the pressure transducers attached to the cylinder of each pump is approximately ± 0.001 MPa. However, the stability of the set pore pressure during flow is strongly dependent on the performance of the servo controller and is decreasing with an increase in flow-rate. Pore pressure fluctuations so induced are approximately ± 0.002 MPa at 2.0 mL/min and ± 0.01 MPa at 20 mL/min. For a permeability measurement, the aim is therefore to choose the lowest flow-rate possible that still yields a significant pressure gradient. For example, a permeability of 10^{-15} m^2 at 150 °C can precisely be resolved with a flow-rate of 0.1 mL/min. When the fluid is pure water the resulting pressure gradient is approximately 0.02 MPa with an uncertainty of 5 %.

In addition to those servo controller related issues the pressure gages of the pumps show an electric drift in their signal – absolute and also relative to each other – over time. Figure 8 shows a typical pressure readout of one of the upstream pumps as a function of time during a continuous flow experiment with a Lower Permian (Rotliegend) sandstone sample. The downward peaks denote an opening of the connection valve between the upstream and the

downstream side of the specimen. The "length" of this peak is then directly equivalent to the pressure difference over the sample. The raw data comprises voltage readouts which can be transformed into pressure values given an appropriate calibration. The latter was performed for all pump pressure transducers against one of the downstream pumps with the stored Isco servo controller calibration taken as the reference. We found this method of taking discontinuous measurements in specific time intervals during a continuous flow experiment the most precise method for determining rock permeability with our apparatus. Drifted pressure values entering the permeability calculation are thus circumvented as the measurement does only rely on the readout of the active upstream pump.
The device is capable of measuring permeabilities over six orders of magnitude ranging from 10^{-18} to 10^{-12} m^2. Higher values are limited by the smallest cross section within the pore fluid system and lower ones, for practical reasons, by the time required to reach steady state. Potentially, transient methods (e.g. the pore pressure pulse technique; Brace et al., 1968) could improve the resolution below 10^{-18} m^2 but they have not yet been explored.

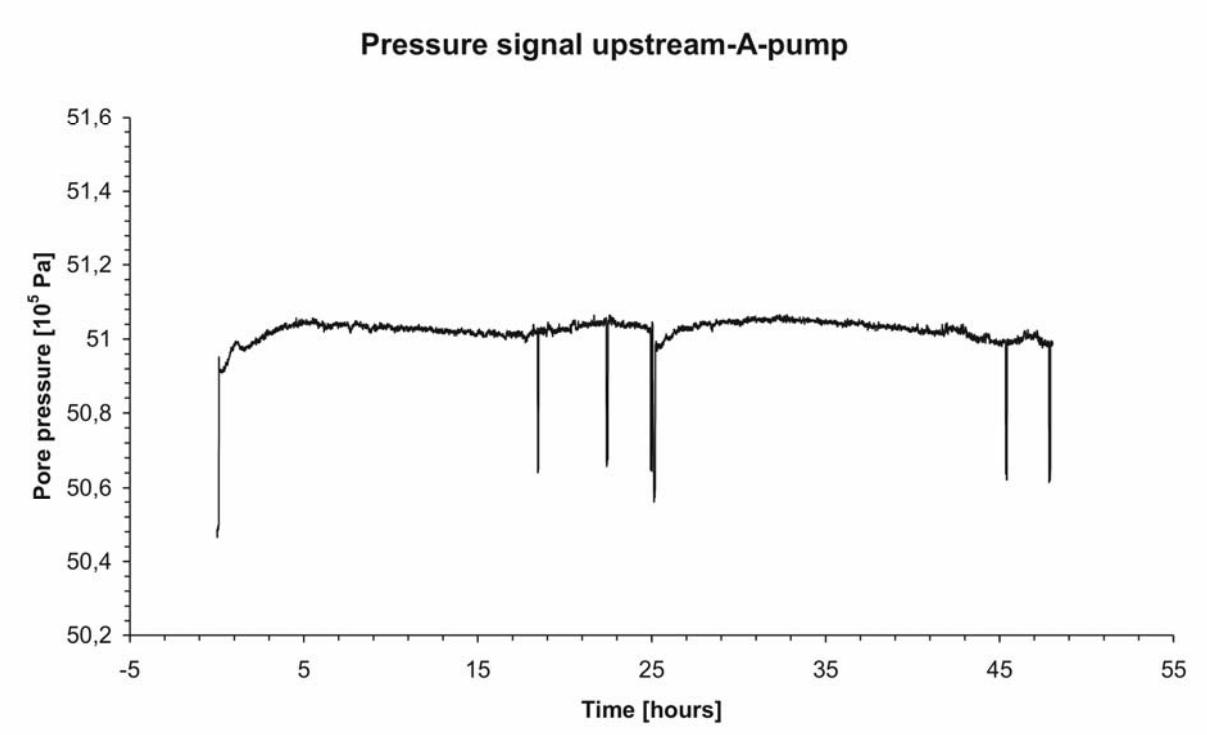

Figure 8. Pore pressure readout during a continuous flow experiment as a function of time measured with one of the upstream pumps. Pressure fluctuations (bold line) are due to electric drift of the pressure transducers. Downward peaks indicate an opening of the connection valve between the up- and the downstream side of the specimen. The peak "length" is directly equivalent to the pressure difference used for calculating the sample permeability.

3b. Electrical conductivity- and ultrasonic measurements

Electrical conductivity measurements are performed in a four-electrode arrangement with a variable shunt-resistor. The voltage measured over the shunt yields the impressed current and is combined with the voltage measured over the distance between the silver rims at the sample. The specific electrical conductivity σ is then given by:

$$\sigma = \frac{d_{Ag}}{R_{sample} \cdot A} = \frac{U_{shunt} \cdot d_{Ag}}{U_{Ag} \cdot R_{shunt} \cdot A}, \quad (4)$$

where R_{sample}, d_{Ag}, A, U_{shunt}, U_{Ag} and R_{shunt} denote, in this order, the sample resistance, the distance between the silver rims, the cross sectional area of the sample, the voltage over the shunt, the voltage between the silver rims and the shunt resistance.
In addition, the frequency dependence of the electrical resistivity of a rock sample can be measured with a commercial impedance spectrometer (Newtons4th Ltd. PSM1700). This device then uses the same four-electrode connections as the measurement at a static frequency described above.
As the rock conductivity in the present experiments is mainly determined by the ionic conductivity of the fluid, temperature fluctuations affect the stability of the measured signal. However, so induced effects can be corrected for if the temperature dependence of the respective fluid viscosity is known (Guéguen and Palciauskas, 1994, p. 189). The remaining uncertainty in the measured electrical conductivity would then be due to noise within the signal generating- and the data acquisition system including the wires which is in the range of ± 0.2 mV. The latter corresponds to an error of only 0.1 % as the typical voltages measured are in the order of 0.2 V. However, the width of the silver rims is in the order of 1.0 mm and thus not negligible with respect to their distance. Errors made in determining the absolute specific electrical conductivity with reference to an exact distance of 25 mm could therefore be as high as 8.0 %. But more importantly, potential relative variations in specific electrical conductivity of an individual sample in the course of an experiment are exact to a much higher extent.
Ultrasonic measurements are made separately for p- and s-waves. The raw data comprises the full waveforms and can be used for further treatment (e.g. instantaneous frequency and spectral energy). Wave velocities can also be directly determined on-screen by reading the travel time from excitation to the first p- or s-wave arrivals. Travel times of the steel plugs have been measured separately for correction.
The time resolution of the oscilloscope is ± 0.1 µs which is approximately the uncertainty in determining the first p- or s-wave arrivals. Thus, for a typical travel time of 20 to 30 µs measured for a sandstone sample of 40 mm length the error in calculating wave velocities is less than 0.5 %. However, it can sometimes be difficult to identify the first s-wave arrival. Thus, cycle skipping by incorrect picking can introduce an additional error in s-wave velocity determination.

4. Discussion and summary

The two identical apparatuses described above with respect to their set-up and performance have been succesfully tested for confining pressures, pore pressures and temperatures of 100 MPa, 50 MPa and 200 °C, respectively. Stress-isotropic upper crustal in-situ conditions down to approximately 4.0 km depth, including the respective temperatures for a normal geothermal gradient, can thus be simulated. In addition, four important petrophysical parameters –

permeability, electrical conductivity as well as p- and s-wave velocities – can be determined simultaneously.
Continuous flow experiments, so far, have been performed over a maximum of six months. Stable physical conditions have thus been maintained over periods that are significantly longer than those usually attained in conventional laboratory based petrophysical testing. In addition, it showed that the use of highly saline formation fluids often found in deep geothermal reservoirs is technically extremely demanding when dynamic seals are involved and also in terms of potential corrosion problems within the pore fluid system despite a thorough material selection.
The scientific outcome of these long-term experiments as well as a review of the observed technical challenges is presented in our companion paper (Milsch et al. in review).

Acknowledgements

The authors are grateful for the technical assistance by the members of the GFZ workshop, namely Peter Stock and Ronny Giese.
This research project is financially supported by the Federal Ministry for the Environment, Nature Conservation and Nuclear Safety under Grant No. BMU 0329951B.

References

Bear, J.: Dynamics of fluids in porous media. Dover Publ., Inc. Mineola, NY (1988).

Brace, W. F., Walsh, J. B., and Frangos, W. T.: Permeability of granite under high pressure. J. Geophys. Res. 73, 2225-2236 (1968).

Civan, F.: Reservoir formation damage – Fundamentals, Modelling, Assessment, and Mitigation. 1st Ed., Gulf Publ. Co., Houston, TX, and Butterworth-Heinemann, Woburn, MA, 742 p. (2000).

Darcy, H.: Les fontaines publique de la ville de Dijon. Dalmont, Paris (1856).

Guéguen, Y. and Palciauskas, V.: Introduction to the physics of rocks. Princeton University Press, Princeton, NJ (1994).

Heiland, J.: Laboratory testing of coupled hydro-mechanical processes during rock deformation. Hydrogeol. J. 11, 122-141 (2003).

Kulenkampff, J., Spangenberg, E., Flovenz, O., Raab, S., and Huenges, E.: Petrophysical parameters of rocks saturated with liquid water at high temperature geothermal reservoir conditions. Proceedings World Geothermal Congress, Antalya, Turkey, paper 1610 (2005).

Leone, J. A. and Scott, M. E.: Characterization and control of formation damage during water flooding of a high-clay-content reservoir. SPE Reservoir Engineering Vol. 3 (1), SPE paper 16234 (1988).

Mader, D.: Hydraulic proppant fracturing and gravel packing. Developments in Petroleum Science 26, Elsevier Science Publishers B. V., The Netherlands (1989).

Milsch, H., Seibt, A., and Spangenberg, E.: Long-term petrophysical investigations on geothermal reservoir rocks at simulated in-situ conditions. Transp. Porous Med (in review) (2007).

Omar, A. E.: Effect of brine composition and clay content on the permeability damage of sandstone cores. J. Petroleum Sci. Eng. 4, 245-256 (1990).

Pape, H., Clauser, C., Iffland, J., Krug, R. and Wagner, R.: Anhydrite cementation and compaction in geothermal reservoirs: Interaction of pore-space structure with flow, transport, P-T conditions, and chemical reactions. Int. J. Rock Mech. Min. Sci. 42 (7-8), 1056-1069 (2005).

Paterson, M. S.: Rock deformation experimentation. In: Duba, A.G., Durham W. B., Handin J. W. and Wang H. F. (eds.) The brittle-ductile transition in rocks. Geophysical Monograph 56, 187-194. AGU, Washington, DC (1990).

Scheidegger, A. E.: The physics of flow through porous media. Univ. of Toronto Press, Toronto (1974).

Sorbie, K. S. and Mackay, E. J.: Mixing of injected, connate and aquifer brines in waterflooding and its relevance to oilfield scaling. J. Petroleum Sci. Eng. 27 (1-2), 85-106 (2000).

Tenthorey, E., Scholz, C. H., Aharonov, E., and Léger, A.: Precipitation sealing and diagenesis: 1. Experimental results. J. Geophys. Res. 103 (B10), 23951-23967 (1998).

Tichstiakov, A. A.: Physico-chemical aspects of clay migration and injectivity decrease of geothermal clastic reservoirs. Proceedings World Geothermal Congress, Kyushu-Tohuko, Japan, 3087-3095 (2000).